

## EVALUATION OF FABRICATED SOLID MICRONEEDLES AS SMART APPROACH FOR TRANSDERMAL DRUG DELIVERY SYSTEM OF ASTAXANTHIN

RAJWANT KAUR<sup>1\*</sup> , SAAHIL ARORA<sup>1</sup> , MANISH GOSWAMI<sup>2</sup> 

<sup>1</sup>University Institute of Pharma Sciences, Chandigarh University, Gharuan, Mohali, Punjab, India. <sup>2</sup>Saraswati Group of Colleges, Gharuan, Mohali, Punjab, India

\*Corresponding author: Rajwant Kaur; \*Email: rajan2286@gmail.com

Received: 20 May 2023, Revised and Accepted: 23 Jun 2023

### ABSTRACT

**Objective:** The lack of drugs to effectively cross the stratum corneum (SC), has recently been a significant barrier to transdermal administration. In order to increase the effectiveness of transdermal distribution, this issue has been solved through the development of micron-scale needles. The objective is to develop, formulate and evaluate biocompatible polymeric solid microneedles with a TDDS-loaded Astaxanthin patch involving the poke and patch method.

**Methods:** The solid microneedle arrays were fabricated using an SLA printer with high-resolution potential and was examined using scanning electron microscopy (25 microns at the *z*-axis and 140 microns at the *x*-axis, respectively). Fabricated Astaxanthin transdermal film was evaluated by many characterization parameters. The developed microneedle was examined for skin insertion and a drug permeation study was carried out across the porcine skin.

**Results:** Solid MN arrays of 1.85  $\mu\text{m}$  tip-to-tip distance, 600  $\mu\text{m}$  height, 300  $\mu\text{m}$  width, and 30  $\mu\text{m}$  tip diameter, were created using biocompatible Class I Dental SG resin. Microneedle crossed stratum corneum layer and penetrated porcine skin with 381.356  $\mu\text{m}$  in depth, with no structural change. Transdermal patches loaded with astaxanthin drug was developed and using various polymer concentration consistent, good, and transparent films were created of thickness between 0.85 $\pm$ 0.07 mm to 0.87 $\pm$ 0.01 mm range, with average weights ranging from 168.02 $\pm$ 1.05 to 172.22 $\pm$ 1.25 10/cm<sup>2</sup>, Folding Endurance with 10-12 folds was reported for formulated transdermal films; also tensile strength was 0.414 $\pm$ 0.002 kg/mm<sup>2</sup> and drug content was 94.41 $\pm$ 0.42% of the best formulation reported. According to studies on drug permeation, Astaxanthin transdermal patches did not significantly permeate porcine skin without being pierced by microneedles the medication exhibited good penetration characteristics.

**Conclusion:** Upon evaluation, formulated transdermal film was reported to be best for solid microneedle-TDDS of astaxanthin for improved patient compliance, bioavailability, and biomedical applications.

**Keywords:** Astaxanthin, Drug delivery, Permeation studies, Solid microneedles, Transdermal

© 2023 The Authors. Published by Innovare Academic Sciences Pvt Ltd. This is an open access article under the CC BY license (<https://creativecommons.org/licenses/by/4.0/>)  
DOI: <https://dx.doi.org/10.22159/ijap.2023v15i5.48421>. Journal homepage: <https://innovareacademics.in/journals/index.php/ijap>

### INTRODUCTION

The lack of drugs to effectively cross the skin stratum corneum barrier has recently been a significant barrier to transdermal administration. In order to increase the effectiveness of transdermal distribution, this issue has been solved through the development of micron-scale needles. Microneedles are painless, minimally invasive techniques that can bypass the SC [1, 2]. They use a combination of hypodermic needles and transdermal patches [3, 4]. Since MNs do not penetrate deeper where there are nerve endings and the SC

lacks nociceptors, they can deliver medications to the permeable portions of skin without inducing pain-related nerves [5-7]. MNs (Microneedles) can also successfully deliver drugs via the intradermal route, avoiding the first pass effect, a significant shortcoming of oral drug administration; drugs with High molecular weight and high water solubility can be administered systemically using this technology. One of the keto carotenoids, astaxanthin having a chemical structure as shown in fig. 1 (3,3-dihydroxy-carotene-4, [4-8], is present in microalga *Haematococcus pluvialis*, red yeast, trout, shrimp, lobster, salmon [9].

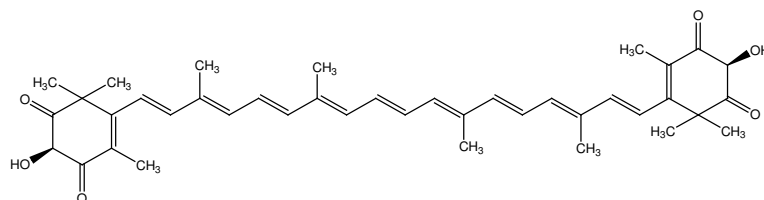


Fig. 1: Structure of astaxanthin

Astaxanthin, one of the carotenoids, is the pigment-producing compound that is soluble in most organic solvents but insoluble in water. Furthermore, according to scientific studies, astaxanthin has cardioprotective benefits, anti-tumor effects, and anti-inflammatory effects in addition to having antioxidant characteristics that are 10 times more potent than those of other carotenoids [10]. Moreover, Astaxanthin has been shown to suppress the synthesis of ROS and

guard bovine oviduct epithelial cells against oxidative stress brought on by NO. MDDS delivers a maximum drug dose without being obstructed by other parameters. As the oral route is the potential degrading route for antioxidants via oxidation or hydroxylation, therefore, a new drug delivery system is also proposed for Astaxanthin. This proposed system is a microneedle-based drug delivery system that is not only devoid of the disadvantages of oral

route and also one step ahead of the benefits of transdermal route. Delivery of Astaxanthin via a microneedle drug delivery system will ensure the availability of Astaxanthin at cellular level and thereby matching the *in vitro* or *ex vivo* correlation to the real effect. In this study, Astaxanthin-loaded solid microneedle patches were evaluated and the impact on drug permeation was assessed using porcine skin. Varying concentrations of Eudragit E-100 and HPMC polymers were used for the formulation of transdermal patch [11].

## MATERIALS AND METHODS

### Materials reagents and chemicals

The Beijing Gingko Group in Beijing, China provided a sample of the drug astaxanthin as a gift. Eudragit E-100, Carbapol 434, Eudragit L-100, Sodium CMC (Carboxymethyl cellulose), and Eudragit RLPO, were procured from Sigma Aldrich, India. Other analytical grade chemicals were procured from Yarrow Chem Limited.

### Methods

#### CADD design furnishing for fabricating microneedles

Using solidwork software, the microneedle array's geometry and orientation were designed as a pyramid and a cone, respectively. Cross sections of solid works are square and circular, respectively [11]. The microneedle had a length of 600  $\mu\text{m}$ , with the base cross sections being 300  $\mu\text{m}$  and the tip being 30  $\mu\text{m}$  apart by 1.85 mm i.e. tip-to-tip. An 11\*11 array patch was attached with a solid 15x15x1 mm substrate to construct the microneedles. As well, the array for fabrication was evaluated using the relevant literature before being generated in an AutoCAD (Autodesk, Cupertino, CA, USA) stl file. The developed 3-Dimensional Microneedles design is displayed in fig. 2.

#### Fabrication of a microneedle array

Dental SG, biocompatible Class-I resin from Form Labs, was selected as the printing medium. Adroitec Pvt. Ltd. employs a stereolithography (SLA) printer to fabricate the arrays; moreover, it is capable of high resolution 25 microns for x-axis and 140 microns for z-axis.

### Transdermal patch formulation

SCT (Solvent casting Technique) was used to fabricate a patch containing astaxanthin in a glass Mould that was made onsite. Using placebo patches, the most efficient polymer, plasticizer, and solvent combinations were evaluated [12-15]. The two compatible polymers, Eudragit E-100 and HPMC were combined for enhanced stability, improved bioavailability and prolonged drug release with a magnetic stirrer, followed by the addition of 20 ml of methanol solvent solution for dissolution. To create a homogeneous solution, progressively drug solution was added to the polymer mixture and well mixed followed by the addition of a plasticizer (polyethylene glycol). As shown in table 1, various polymer ratios were trying to develop patches. The developed transdermal patches were also assessed for a number of characterization tests [16, 17].

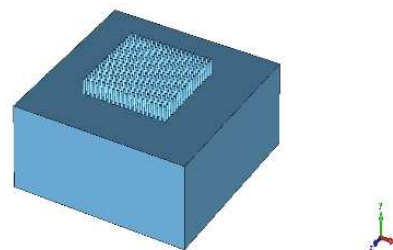


Fig. 2: Developed 3D array of microneedles

### Characterization studies

#### Examining drug-polymer compatibility

To assess the compatibility of drugs and polymers, the FTIR of Astaxanthin and polymer mixtures were evaluated. Data covering the spectral range of 450-4000  $\text{cm}^{-1}$  was obtained upon sample treatment with KBr [18].

Table 1: Design of astaxanthin transdermal film

TDDS formulation No.	HPMC (mg)	Eudragit e-100 (mg)	Permeation enhancer (ginger oil in ml)	Methanol (ml)	Plasticizer (polyethylene glycol in %)	Drug (mg)
AXT-1	50	500	0.5	20	2	4
AXT-2	100	400	0.5	20	2	4
AXT-3	200	300	0.5	20	2	4
AXT-4	300	200	0.5	20	2	4
AXT-5	400	100	0.5	20	2	4
AXT-6	500	50	0.5	20	2	4

### SEM study

To evaluate the needles' dimensions, shape, and other physical characteristics, the morphology of microneedle patches was examined using a low-speed acceleration voltage SEM (scanning electron microscopy) utilizing a Hitachi SU 8030, Japan (1.0kV). A low accelerating voltage was used in order to prevent electrical currents from building up on the cross microneedles. At different magnifications, coated cross-microneedles were digitally captured from a specific working distance [19].

#### Thickness and weight variation of formulated transdermal film

Fabricated MN and transdermal patch were measured for consistency of thickness using a digital micrometer screw gauge. The analysis of weight variation was accomplished by individually weighing patches selected at random, and random micrometer measurements of film thickness were taken of all formulated films [20].

#### Drug content determination

A 1  $\text{cm}^2$  transdermal film that contained 4 mg of the drug was dissolved in pH-7.4 phosphate buffer and stirred repeatedly for 24 h. for drug

extraction from the film. After filtering and phosphate buffer dilution, the quantity of drug contained was assessed via spectra at 482.0 nm [21].

#### Flatness

A flatness assessment was carried out to make sure the formulated film had a smooth surface and will not shrink with time. Three longitudinal strips, each cut at a different point, were cut out of the film [21]. A percent constriction scale, where 0% constriction equals 100% flatness, was used to measure the length of each strip as well as the variation in length brought on by non-uniformity in flatness.  $(L_1 - L_2) / L_1 * 100$  was the formula for percent constriction. Thus, each strip has a length of  $L_1$  at the start and  $L_2$  at the end.

#### Folding endurance and tensile strength

The number of times the film could be folded in the same place without rupturing was used to determine the folding endurance rating. The tensile strength was determined using a tensiometer.

#### Moisture content and moisture uptake

The fabricated patch was individually weighed and then managed to keep in desiccators with activated  $\text{CaCl}_2$  solutions for 24 h, to

calculate the percentage of moisture content and moisture uptake, respectively.

#### Comparative studies conducted *in vitro* on MN poked skin and whole skin

Porcine ears from recently sacrificed pigs were collected from a local slaughterhouse. The outer layer was detached after being cleaned

with ice-cold deionized water by the skin grafting handle. It was chosen to use full-thickness, non-dermatomed skin.

As shown in fig. 3, a piece of skin of 1 mm thickness was placed on the Franz diffusion cell. The permeation studies were used to calculate the drug's flux and permeability coefficient. Pig ear skin was used in skin permeation studies because it exhibits permeability characteristics that are comparable to those of human skin.



Fig. 3: Mounted porcine skin samples for permeation studies using a franz diffusion cell

The modified franz diffusion cell setup was used to quantify the amount of astaxanthin that permeated through the skin of pig ears. The donor compartment in the test equipment had a capacity of 3.319 cm<sup>3</sup> and an area of about 1.3263 cm<sup>2</sup>, according to calculations. As receptor media, pH 7.4 phosphate buffer was utilized, and throughout the trials, water circulation and stirring at a set RMP were used to maintain receptor media at 37.5 °C [22]. The donor compartment's skin surface was covered with a 100% saturated solution of astaxanthin that had been made in the aforementioned conditions and sealed with parafilm to prevent air influence. To measure the drug's permeability over the skin, 1 ml of aliquots were obtained from the receptor compartment at intervals ranging from 0 h to 24 h. The receptor received an equivalent amount of media for each withdrawn sample. In order to fulfill the statistical criteria, further astaxanthin dilutions in the range of 10%, to 90% were prepared involving a triplicate study [23].

For comparative studies, steady state flux was to be calculated for microneedle poked skin samples. Skin samples were prepared for study. On a platform made of polystyrene foam, skin samples were placed and Microneedle arrays were manually applied at the centre of the porcine skin. Microneedle arrays were rotated at around 90 ° prior to each reinsert. On the Franz diffusion cell, a section of skin was placed with a 1 mm thickness. The permeability coefficient and flux were determined using the permeation studies.

The modified franz apparatus was used to determine the quantity of astaxanthin that permeated through the skin of pig ears. The donor compartment in the test equipment had a capacity of 3.319 cm<sup>3</sup> and an area of about 1.3263 cm<sup>2</sup>, according to measurements. As receptor media, pH 7.4 phosphate buffer was utilized, and throughout the trials, water circulation and stirring at a set RMP to maintain a temperature of 37.5 °C of the receptor media.

The donor compartment's skin surface was covered with a 100% saturated solution of astaxanthin that had been made in the aforementioned conditions and sealed with parafilm to prevent air influence. To measure the drug's permeability over the skin, approx. 1 ml of aliquots were obtained from the receptor compartment at intervals ranging from 0 h to 24 h. The receptor was filled with an identical amount of media for each withdrawn aliquot. In order to

fulfill the statistical criteria, further astaxanthin dilutions from 10% to 90% were done. Finally, the triplicate result was collected. For comparative studies, readings were taken and steady-state flux was calculated for both whole-skin and microneedle-poked skin samples.

#### Microneedle penetration in porcine skin

Research on *in vitro* skin implantation employed porcine skin of pigs that was rapidly collected after pigs were killed at a nearby slaughterhouse. Porcine skin was cleaned using ice-cold water and then the impacted skin was scraped off. To create full-thickness skin membranes, the whole skin was removed from the cartilage beneath. Before the diffusion testing, defrosted skin was cut into 2\*2 cm squares. The skin samples were firmly fastened using thumbtacks prior to the surface of the microneedle arrays adhering, equivalent to putting a stamp into an envelope or a lift button with force, the skin was physically treated with microneedles for 30 sec. After that, the compression site was pulled off and given a minute-long exposure to a fluorescent dye. The leftover dye was removed from skin samples that were processed for histological examination. For histology specimen preparations, the skin was fixed in formalin, dried, and combined with paraffin. Methylene blue dye was used to colour skin samples, which were then examined using an olympus fluorescence microscope. to gauge penetration depth as reported in fig. 11.

#### RESULTS AND DISCUSSION

Microneedle arrays in the forms of pyramidal and conical have been successfully manufactured using stereolithography, an additive manufacturing technique. Utilizing a biocompatible resin of Class-I, the SLA constructs structures using CAD models as a starting point.

Among the few readily available, FDA-approved polymers is Class-I polymer acceptable for form 2 technologies and stereolithography printers is Dental SG resin. As shown in fig. 3, the Microneedle patches were created by SLA. SLA is a well-liked method for MN fabrication because of the inexpensive printing medium and speed for the production of objects. Quantitatively, the currently available SLA machines for commercial use have a limited print capacity; however employing the recommended dimensions and method, up to 49 MN arrays may be created in approx. 2h with the existing print volume (145\*145\*175 mm). For the technique to be scaled up on an industrial

scale, printers with bigger print volumes must be deployed. However, because of the cheap cost and speedy fabrication of these printers, simultaneous printing in a number of printers may efficiently and accurately create a huge number of arrays.

#### Analysis of astaxanthin by FTIR spectroscopic data

Astaxanthin shows O-H stretching at  $3448\text{ cm}^{-1}$  and carbonyl group at  $1744\text{ cm}^{-1}$ . Further, its C-H stretch was detected at  $2931\text{ cm}^{-1}$  while alcoholic C-O Stretch was found at  $1068\text{ cm}^{-1}$ , which confirms the purity and structure of Astaxanthin. In the IR graph of HPMC, the hydrogen-bonded hydroxyl group was identified at  $3465\text{ cm}^{-1}$  while the C-O stretch was found at  $1057\text{ cm}^{-1}$  and a peak was observed at  $2901\text{ cm}^{-1}$  for C-H Stretch. In Eudragit E-100, the stretching peak of the esteric carbonyl group was found to be  $1725\text{ cm}^{-1}$  and the C-O stretch was visible at  $1150\text{ cm}^{-1}$ . C-H stretch vibrations were obtained at  $2955\text{ cm}^{-1}$ . FTIR analysis of the drug individually of Astaxanthin and astaxanthin with Eudragit and HPMC *i.e.* drug-polymer mixture (fig. 5, 6, 7) reported that the excipients employed did not interact chemically with the drug. With no indication of chemical interaction, variations in the peak area might result from simple component mixing alone [24].



Fig. 4: Fabricated microneedles

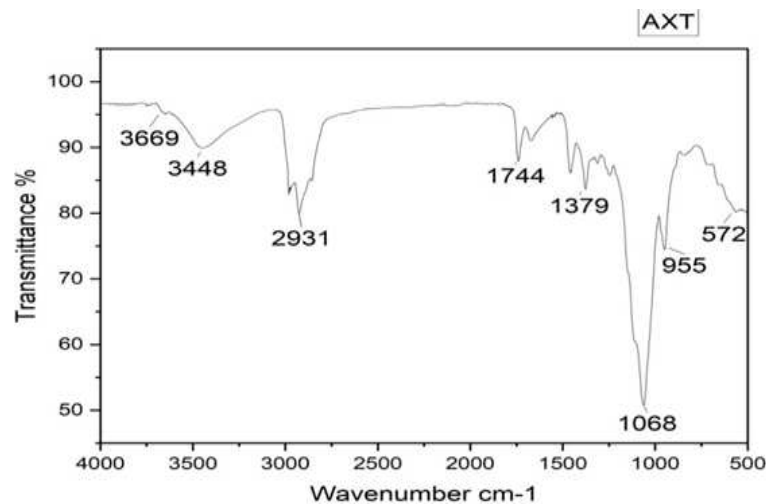


Fig. 5: FTIR spectra of astaxanthin

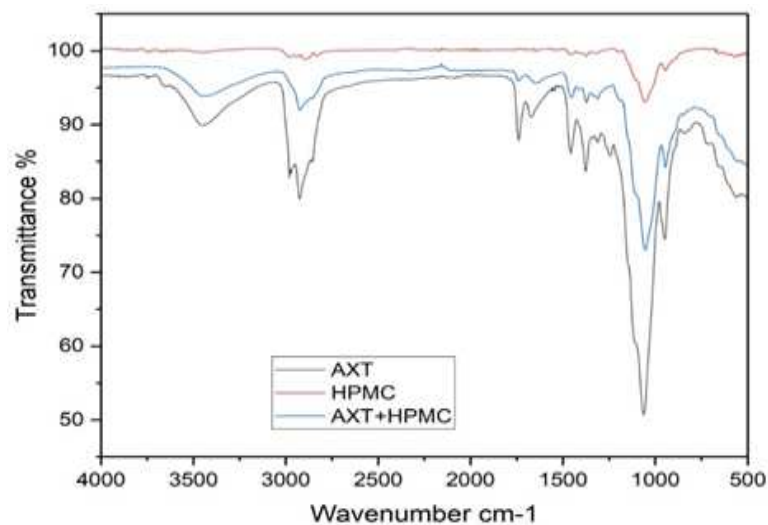


Fig. 6: FTIR spectra of Astaxanthin and HPMC

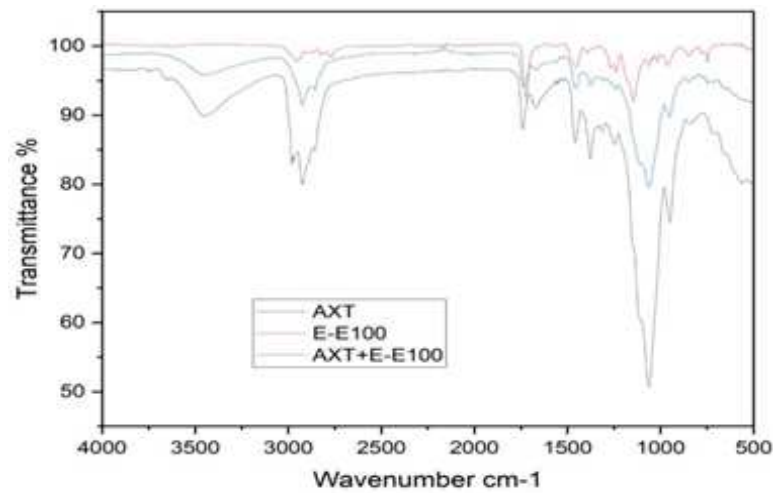


Fig. 7: FTIR spectra of astaxanthin and eudragit E-100

#### Scanning electron microscopy of fabricated microneedle

The scanning electron microscope was used to study fabricated microneedles. According to SEM investigations, each microneedle of height 600  $\mu\text{m}$ , width of 300  $\mu\text{m}$ , 30  $\mu\text{m}$  tip diameter, and tip to tip distance 1.85 mm, as seen in fig. 8. The high resolution of the printer made it possible to regularly build incredibly intricate arrays, which resulted in pointed needle tips that are more suitable for skin implantation [25].

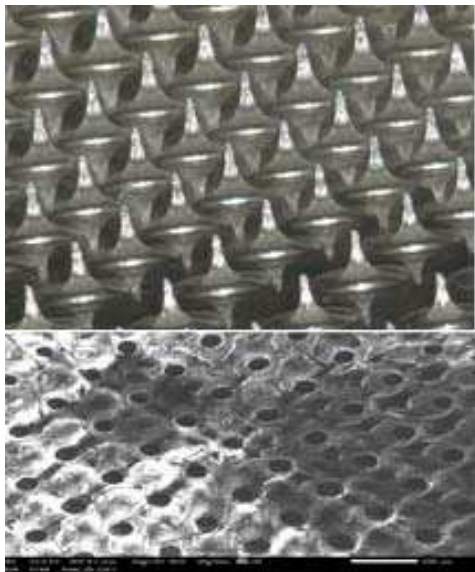


Fig. 8: SEM analysis of fabricated microneedle

#### Evaluation of fabricated transdermal films

The combination of Eudragit E-100 and HPMC with resulted in good, uniform, and clear transdermal films also plasticizer was added to lessen the brittleness in order to make a transdermal film with high elasticity, as discussed in prior studies. The thickness of the fabricated patch was consistently between  $0.83 \pm 0.08$  mm for AXT-4 to  $0.62 \pm 0.01$  mm for AXT-3 upon measured using a micrometer. These findings made it evident that the patch's thickness increases as Eudragit E-100 concentration increased. It means that using the appropriate polymer is necessary for creating patches with the ideal thickness; otherwise, the release of drugs from the patch may be delayed. The average weights were between  $503.55 \pm 2.05$  and  $5011.22 \pm 1.25$  ( $10/\text{cm}^2$ ), demonstrating comparable weights. The prepared patches possessed the strength and flexibility to withstand the mechanical strain, as evidenced by the folding endurance being larger than 11, which was found to be greater than 11. High values of folding endurance were reported in the formulations that contain HPMC [26]. All of the formulations had good drug content; however, AXT-3 had the greatest level with a value of  $94.41 \pm 0.42\%$  and AXT-1 had the lowest with a value of  $89.15 \pm 0.31\%$ . As there was no eruption and no rough spots on any of the prepared patches, the surface was completely flat. The study revealed that the patch fabrication was able to provide patches with a predictable drug concentration and minor variability. The results of investigations on the patches' tensile strength and folding endurance showed that they would not fracture and would maintain their integrity throughout regular skin folding [27]. Tensile strength was discovered to be consistent across all formulations, falling between  $0.330 \pm 0.03$  to  $0.414 \pm 0.02$ , further demonstrating the consistency of transdermal patches. The moisture content that exists between each patch varies between  $1.5 \pm 0.2$  and  $3.2 \pm 0.2$ , with AXT-5 displaying the highest moisture content and AXT-3 having the lowest. Table 2 displays the outcomes of the physicochemical characterization of patches [28].

Table 2: Physical chemical characterization of formulated transdermal film

TDDS formulation No.	Average weight ( $10/\text{cm}^2$ )	Thickness (mm)	Drug content (%)	Folding endurance	Flatness (%)	Tensile strength ( $\text{kg}/\text{mm}^2$ )	Moisture content (%)
AXT-1	$510.02 \pm 1.05$	$0.85 \pm 0.07$	$89.15 \pm 0.31$	$80 \pm 3.1$	$100 \pm 0$	$0.355 \pm 0.04$	$3.2 \pm 0.1$
AXT-2	$504.12 \pm 2.23$	$0.87 \pm 0.09$	$91.28 \pm 0.24$	$99 \pm 3.2$	$100 \pm 0$	$0.417 \pm 0.01$	$2.6 \pm 0.2$
AXT-3	$506.23 \pm 2.61$	$0.62 \pm 0.01$	$94.41 \pm 0.42$	$110 \pm 3.0$	$100 \pm 0$	$0.414 \pm 0.02$	$1.5 \pm 0.2$
AXT-4	$503.55 \pm 2.05$	$0.83 \pm 0.08$	$92.85 \pm 0.47$	$101 \pm 3.2$	$100 \pm 0$	$0.330 \pm 0.03$	$2.8 \pm 0.4$
AXT-5	$5011.22 \pm 1.25$	$0.87 \pm 0.01$	$91.98 \pm 0.34$	$103 \pm 3.1$	$100 \pm 0$	$0.455 \pm 0.04$	$3.2 \pm 0.2$

( $n=3$ , mean $\pm$ SD; experiments were conducted in triplicate)

The minimum release was observed in formulation AXT-1 while the largest release was seen in formulation AXT-3 because of variation in polymer ratio. The longer retention period and improved dissolving are responsible for the greater release in the AXT-3 formulation. Although there is no discernible variation in the formulation's polymer concentration, the optimal concentration of HPMC and Eudragit lengthened the time it took for the medicine to dissolve [25].

**Microneedle penetration in porcine skin**

The prepared array of Microneedles was inserted into pig skin samples using a texture analyzer. The MN designs all succeeded in penetrating the skin; none of them failed. Force against displacement measurements was continually noted throughout the penetration. Without breaking or creating any structural alterations, the microneedles were able to pass through 381.356m depth through the SC layer of pig skin.

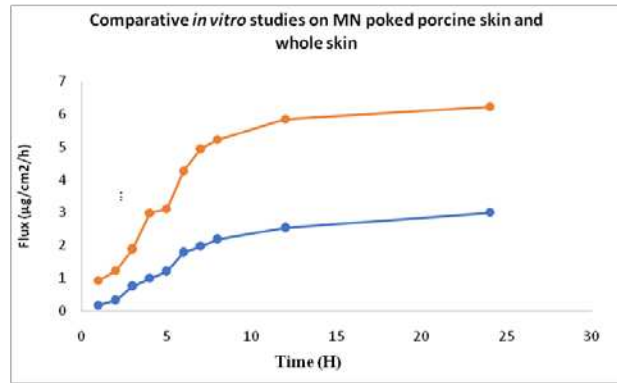


**Fig. 9: Comparative *in vitro* permeation profile of Astaxanthin**

**Comparative studies conducted *in vitro* on MN poked skin and whole skin**

For both MN poked and whole skin, the cumulative amount of each drug penetrating the excised whole-thickness porcine skin has been demonstrated as a function of time. Using linear regression analysis, the slope and intercept of the linear component were determined. The linear component of the cumulative amount versus the time curve was used to compute the steady-state flux. Additionally, the total quantity of each

chemical that penetrated for 24 h was determined. Upon comparative *in vitro* study between poked and whole porcine skin, it was observed the loaded drug molecules entered the body through micropores efficiently as shown in fig. 9. According to the comparative studies' results, MNs significantly affect the transdermal penetration of drugs in contrast to investigations on drug absorption across the whole skin. Additionally, MN's technology is easy to use, convenient, and more patient-acceptable [29, 30]. Fig. 10 shows the 40X microscopic image of fabricated microneedles piercing pig skin under study.

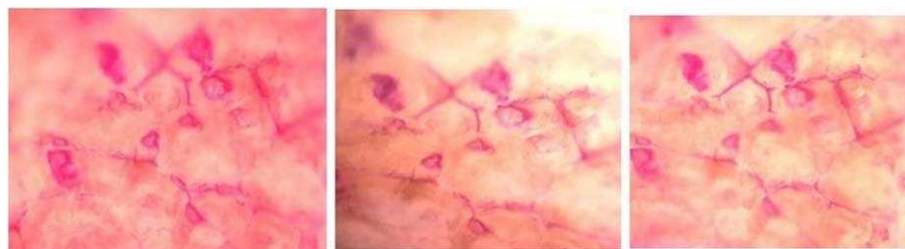


**Fig. 10: Using fabricated MN, a Microscopic Image of poked pig ear skin**

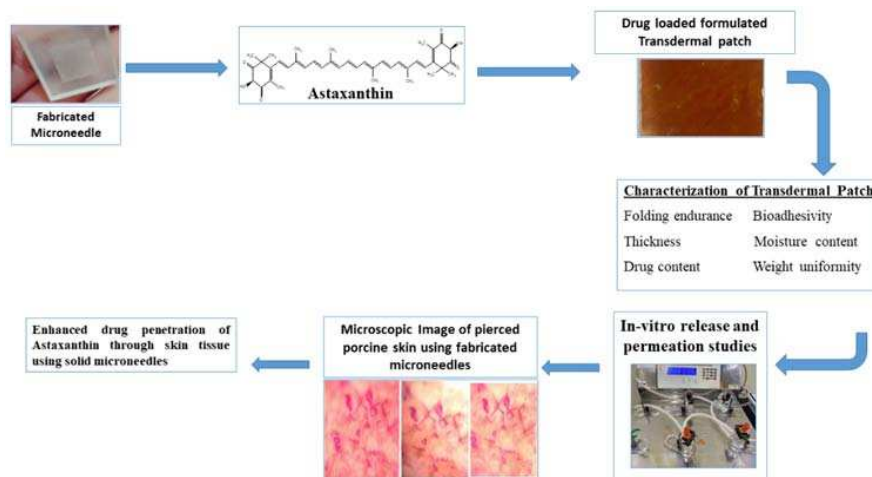


**Fig. 11: Formulated transdermal patch of astaxanthin and solid microneedle combination for improved drug delivery**

The findings of the combined trials demonstrate that MNs, which are painless, easier to apply, and more palatable to patients, have a considerable impact on the transdermal penetration of medications, as shown in fig. 11. Moreover, mechanistic investigations have demonstrated that MNs facilitate transdermal drug penetration by rupturing the SC barrier, whereas microneedle holes just improve drug diffusion without changing the drug-skin interaction.

## CONCLUSION

A microneedle that can fulfill the need to penetrate human skin while preventing injury to the skin and the needle itself was fabricated. In this research, the transdermal flux values for astaxanthin increased statistically significantly when a microneedle was introduced across porcine skin. SEM studies were done to characterize the shape and size of microneedles. *In vitro* permeation tests utilizing solid microneedles, the mean cumulative quantity of drug absorbed through the skin for 24 h was substantially higher than untreated whole skin samples. This shows that the fabricated microneedle may be utilized to make microchannels in the SC and is capable of improving *in vitro* transport of our drug of interest through the skin. Astaxanthin transdermal films have been successfully developed to ensure excellent quality and uniformity in patch characteristics with the least amount of variability, according to the evaluation of the prepared films in terms of physical appearance, weight uniformity, thickness uniformity, surface pH, flatness test, and drug content uniformity.

## ABBREVIATIONS

MNs-Microneedles, AXT-Astaxanthin, TDDS-Transdermal drug delivery system, SC-Stratum corneum, MDDS-Microneedle drug delivery system

## FUNDING

Nil

## AUTHORS CONTRIBUTIONS

Rajwant Kaur, Saahil Arora, and Manish Goswami conceived the presented idea. Rajwant Kaur and Saahil Arora developed the theory and completed the research work. Saahil Arora verified the analytical methods. Dr. Manish Goswami supervised the findings of this work. All authors discussed the results and contributed to the final manuscript.

## CONFLICT OF INTERESTS

Declared none

## REFERENCES

- Mikszta JA, Alarcon JB, Brittingham JM, Sutter DE, Pettis RJ, Harvey NG. Improved genetic immunization via biomechanical disruption of skin barrier function and targeted epidermal delivery. *Nat Med*. 2002;8(4):415-9. doi: 10.1038/nm0402-415, PMID 11927950.
- Donnelly RF, Raj Singh TR, Woolfson AD. Microneedle-based drug delivery systems: microfabrication, drug delivery, and safety. *Drug Deliv*. 2010;17(4):187-207. doi: 10.3109/10717541003667798, PMID 20297904.
- Sharma C, Thakur N, Goswami M. Penetration enhancers in current perspective. *Ann Trop Med Public Heal*. 2020;23(15). doi: 10.36295/ASRO.2020.231527.
- Sharma C, Thakur N, Kaur B, Goswami M. Transdermal patches: state of the art. *Int J Drug Deliv Technol*. 2020;10(3):414-20. doi: 10.25258/ijddt.10.3.19.
- Larraneta E, Lutton REM, Woolfson AD, Donnelly RF. Microneedle arrays as transdermal and intradermal drug delivery systems: materials science, manufacture and commercial development. *Materials Science and Engineering: R: Reports*. 2016;104:1-32. doi: 10.1016/j.mser.2016.03.001.
- Tiwari A, Sharma S, Soni PK, Paswan SK. Fabrication and development of dissolving microneedle patch of butorphanol tartrate. *Int J App Pharm*. 2023;15(3):261-71. doi: 10.22159/ijap.2023v15i3.47411.
- Sachdeva V, Banga AK. Microneedles and their applications. *Recent Pat Drug Deliv Formul*. 2011;5(2):95-132. doi: 10.2174/187221111795471445, PMID 21453248.
- Higuera Ciapara I, Felix Valenzuela L, Goycoolea FM. Astaxanthin: a review of its chemistry and applications. *Crit Rev Food Sci Nutr*. 2006;46(2):185-96. doi: 10.1080/10408690590957188, PMID 16431409.
- Ambati RR, Phang SM, Ravi S, Aswathanarayana RG. Astaxanthin: sources, extraction, stability, biological activities and its commercial applications-a review. *Mar Drugs*. 2014;12(1):128-52. doi: 10.3390/md12010128, PMID 24402174.
- Leung LYL, Chan SMN, Tam HL, Wong ESW. Astaxanthin influence on health outcomes of adults at risk of metabolic syndrome: a systematic review and meta-analysis. *Nutrients*. 2022;14(10):2050. doi: 10.3390/nu14102050, PMID 35631193.
- Rypl D, Bittnar Z. Generation of computational surface meshes of STL models. *J Comput Appl Math*. 2006;192(1):148-51. doi: 10.1016/j.cam.2005.04.054.
- Kaur B, Thakur N, Goswami M. Evaluating the impact of solid microneedles on the transdermal drug delivery system for  $\gamma$ -Oryzanol. *Int J Appl Pharm*. 2022;14(6):34-41.
- Sharma C, Thakur N, Kaur B, Goswami M. Investigating effects of permeation enhancers on percutaneous absorption of loxapine succinate. *Int J App Pharm*. 2022;14(4):158-62. doi: 10.22159/ijap.2022v14i4.44896.
- Thakur N, Kaur B, Sharma C, Goswami M. Evaluation of the dermal irritation and skin sensitization due to thiocolchicoside transdermal drug delivery system. *Int J Health Sci*. 2022;6(Mar):3057-66. doi: 10.53730/ijhs.v6n3.6274.
- Thakur N, Kaur B, Goswami M, Sharma C. Compatibility studies of the thiocolchicoside with Eudragit RLPO, Eudragit E100 and Eudragit L100 using thermal and non-thermal methods. *Drug Comb Ther*. 2022;4(1):1-9. doi: 10.53388/DCT2021100301.
- Qothrunnadaa T, Hasanah AN. Patches for acne treatment: an update on the formulation and stability test. *Int J App Pharm*. 2021;13(4):21-6. doi: 10.22159/ijap.2021.v13i4.43812.
- Patel KN, Patel HK, Patel VA. Formulation and characterization of the drug in adhesive transdermal patches of diclofenac acid. *Int J Pharm Pharm Sci*. 2012;4(1):296-9.
- Rastogi V, Yadav P. Transdermal drug delivery system: an overview. *Asian J Pharm*. 2012;6(3):161-70. doi: 10.4103/0973-8398.104828.
- Kumar CA, Ashwini J, Archana GL, Laxmi SV, Garige AK, Chandupatla V. Transdermal patches for the treatment of angina pectoris: an effective drug delivery system-a review. *Int J App Pharm*. 2022;14(4):115-25. doi: 10.22159/ijap.2022v14i4.44623.
- Shivalingam MR, Balasubramanian A, Ramalingam K. Formulation and evaluation of transdermal patches of pantoprazole sodium. *Int J App Pharm*. 2021;13(5):287-91. doi: 10.22159/ijap.2021v13i5.42175.
- Ravi G, Gupta NV. Development and evaluation of transdermal film containing solid lipid nanoparticles of rivastigmine tartrate. *Int J App Pharm*. 2017;9(6):85-90. doi: 10.22159/ijap.2017v9i6.22354.
- Sarwar Z, Farooq M, Adnan S, Saleem MU, Masood Z, Mahmood A. Development and optimization of metoclopramide containing polymeric patches: impact of permeation enhancers. *Braz J Pharm Sci*. 2022;58:1-19. doi: 10.1590/s2175-97902022e21131.
- Narula A, Sabra R, Li N. Mechanisms and extent of enhanced passive permeation by colloidal drug particles. *Mol Pharm*. 2022;19(9):3085-99. doi: 10.1021/acs.molpharmaceut.2c00124, PMID 35998304.
- Monika B, Amit R, Sanjib B, Alisha B, Mihir P, Dhanushram T. Transdermal drug delivery system with formulation and evaluation aspects: overview. *Res J Pharm Technol*. 2012;5(9):1168-76.
- Kumar M, Trivedi V, Shukla AK, Dev SK. Effect of polymers on the physicochemical and drug release properties of transdermal patches of atenolol. *Int J App Pharm*. 2018;10(4):68-73. doi: 10.22159/ijap.2018v10i4.24916.
- Shehata TM, Mohafez OMM, Hanieh HN. Pharmaceutical formulation and biochemical evaluation of atorvastatin

- transdermal patches. *Indian J Pharm Educ Res.* 2018;52(1):54-61. doi: 10.5530/ijper.52.1.6.
27. Mittal A, Sara UV, Ali A. Formulation and evaluation of monolithic matrix polymer films for transdermal delivery of nitrendipine. *Acta Pharm.* 2009;59(4):383-93. doi: 10.2478/v10007-009-0032-9, PMID 19919928.
  28. Anod HV, Gupta NV, Gowda DV, MM. Preparation and evaluation of simvastatin transdermal film. *Int J App Pharm.* 2018;10(5):235-8. doi: 10.22159/ijap.2018v10i5.26657.
  29. Milewski M, Yerramreddy TR, Ghosh P, Crooks PA, Stinchcomb AL. *In vitro* permeation of a pegylated naltrexone prodrug across microneedle-treated skin. *J Control Release.* 2010;146(1):37-44. doi: 10.1016/j.jconrel.2010.05.034, PMID 20678989.
  30. Sethi B, Mazumder R. Comparative evaluation of selected polymers and plasticizer on transdermal drug delivery system. *Int J App Pharm.* 2018;10(1):67-73. doi: 10.22159/ijap.2018v10i1.21960.